



TITLE:

Detection of phase separation of neutron-irradiated Fe–Cr binary alloys using positron annihilation spectroscopy

AUTHOR(S):

Noshita, Y.; Sato, K.; Yamashita, H.; Kasada, R.; Xu, Q.; Hatakeyama, M.; Sunada, S.

---

CITATION:

Noshita, Y. ...[et al]. Detection of phase separation of neutron-irradiated Fe–Cr binary alloys using positron annihilation spectroscopy. Nuclear Materials and Energy 2018, 15: 175-179

ISSUE DATE:

2018-05

URL:

<http://hdl.handle.net/2433/233864>

RIGHT:

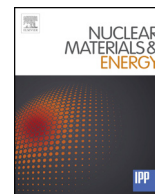
© 2018 Elsevier Ltd. This is an open access article under the CC BY-NC-ND license (<http://creativecommons.org/licenses/by-nc-nd/4.0/>).



Contents lists available at ScienceDirect

# Nuclear Materials and Energy

journal homepage: [www.elsevier.com/locate/nme](http://www.elsevier.com/locate/nme)



## Detection of phase separation of neutron-irradiated Fe–Cr binary alloys using positron annihilation spectroscopy

Y. Noshita<sup>a</sup>, K. Sato<sup>a,\*</sup>, H. Yamashita<sup>a</sup>, R. Kasada<sup>b</sup>, Q. Xu<sup>c</sup>, M. Hatakeyama<sup>d</sup>, S. Sunada<sup>d</sup>

<sup>a</sup> Graduate School of Science and Engineering, Kagoshima University, Korimoto, Kagoshima 890-0065, Japan

<sup>b</sup> Institute for Materials Research, Tohoku University, Katahira, Aoba-ku, Sendai 980-8577, Japan

<sup>c</sup> Research Reactor Institute, Kyoto University, Kumatori-cho, Sennan-gun, Osaka 590-0494, Japan

<sup>d</sup> Graduate School of Science and Engineering for Research, University of Toyama, Gofuku, Toyama 930-8555, Japan

### ARTICLE INFO

#### Keywords:

Fe–Cr binary alloys  
Neutron irradiation  
Positron annihilation  
Hardness  
Phase separation

### ABSTRACT

Phase separation in Fe–Cr binary alloys irradiated with neutrons at 473 K and 573 K was investigated using positron annihilation spectroscopy. Using positron annihilation coincidence Doppler broadening (CDB) measurements, the phase separation progress was observed in neutron-irradiated samples at 473 K and 573 K. Vacancy clusters were detected in Fe–xCr ( $x = 0, 9, 15, 30, 45, 50$ , and  $100$ ) during 473 K irradiation using positron annihilation lifetime measurements, but were not detected in Fe–xCr ( $x = 70, 85$ , and  $91$ ) irradiated at 473 K or in any samples irradiated at 573 K. Additionally, in Fe–xCr ( $x = 70, 85$ , and  $91$ ) irradiated at 473 K, all positrons were annihilated with core Fe electrons as determined from CDB ratio curves. Thus, vacancy clusters were not detected in the Fe-rich phase. There was a possibility that vacancy clusters are formed in the Cr-rich phase, but they were not detected by the PAS. Therefore, another method is necessary to investigate this further. Vickers hardness tests indicated that neutron-irradiated samples were harder than unirradiated samples. The contribution of phase separation and neutron-irradiation defects to increased hardness was dependent on the irradiation conditions including temperature and dose.

### 1. Introduction

Ferritic stainless and heat-resistant steels used as peripheral materials in nuclear reactors possess high Cr content [1]. In these materials, ductility and toughness decrease significantly while hardness and tensile strength increase as the material is aged from 593 to 813 K [2]. Akita et al. reported that hardness in ferritic stainless steels (SUS430, SUS444, SUS447) increased after aging at 673–793 K for 100 h [3]. This is caused by the formation of Fe-rich and Cr-rich phases, a phenomenon called 475 °C embrittlement [4]. These changes in mechanical properties are important when evaluating aging-induced deterioration when the materials are used as structural materials in reactors. The phase separation process of Fe–Cr binary alloys has been studied with multiple techniques. The formation of the Cr-rich phase was detected in Fe–xCr ( $x = 21, 29, 36$ , and  $55$  at.%) aged at 748 K for 5000 h using Mössbauer spectroscopy [5–7]. Brenner et al. also detected the formation of the Cr-rich phase in Fe–32at.%Cr aged at 743 K using a field-ion microscopy and atom-probe analysis [8].

After neutron irradiation above 523 K, the Cr-rich phase was formed even in the ferritic stainless steels (Cr content:  $> 8$  wt.%), which was detected by the small-angle neutron scattering technique [9]. The

distribution of dislocation loops induced by the neutron irradiation at 573 K was heterogeneous, which was influenced by the formation of the Cr-rich phase [10]. Chen et al. detected phase separation in Fe–9.7%Cr irradiated with neutrons at 573 K by atom probe tomography [11]. Excessive irradiation-induced defects promoted phase separation even at temperatures less than 593 K.

Positron annihilation spectroscopy (PAS) is an extremely powerful tool for obtaining information on vacancy-type defects, including single vacancies and precipitates. Xu et al. reported the positron annihilation lifetimes of vacancy clusters and the change in spectra via coincidence Doppler broadening (CDB) in association with the formation of Cu precipitates in neutron-irradiated Fe–Cu alloys [12]. Positrons are trapped in clusters of elements and embedded phases that have more negative positron affinity than that of the matrix. In the Fe–Cr alloys used in this study, the Fe positron affinity is more negative than that of Cr [13]. Therefore, we can detect the formation of an Fe-rich phase by the phase separation of Fe–Cr alloys using PAS. The purpose of this study is to detect the progress of phase separation using PAS and to obtain a correlation between the hardness and phase separation in Fe–Cr binary alloys irradiated with neutrons at 473 K and 573 K.

\* Corresponding author at: Graduate School of Science and Engineering, Kagoshima University, Kagoshima-shi, Kagoshima, 890-0065 Japan.  
E-mail address: [ksato@mech.kagoshima-u.ac.jp](mailto:ksato@mech.kagoshima-u.ac.jp) (K. Sato).

**Table 1**  
Chemical composition of samples used in this study.

Sample	Composition (wt.%)			
	Cr	C	O	N
Fe		<0.001	0.0035	<0.0005
Fe–9Cr	8.84	<0.001	0.0081	<0.0005
Fe–15Cr	15.1	0.001	0.0064	<0.0005
Fe–30Cr	29.7	0.001	0.012	<0.0005
Fe–45Cr	44.9	0.001	0.016	<0.0005
Fe–50Cr	49.5	0.001	0.015	<0.0005
Fe–70Cr	68.3	0.057	0.0015	0.0017
Fe–85Cr	83.1	0.001	0.024	<0.0005
Fe–91Cr	90.95	<0.001	0.027	<0.0005
Cr		0.001	0.028	<0.0005

## 2. Experimental procedure

Fe– $x$  wt.%Cr ( $x = 0, 9, 15, 30, 45, 50, 70, 85, 91$ , and 100) binary alloys were used in this study; their chemical compositions are shown in Table 1. The weights of high purity Fe (99.99%) and Cr (99.99%) were measured and samples were melted by arc melting. For homogenization, Fe– $x$ Cr ( $x = 0, 9, 15, 30, 45$ , and 50) were annealed at 1273 K for 24 h in a vacuum ( $< 4 \times 10^{-4}$  Pa), and Fe– $x$ Cr ( $x = 70, 85, 91$ , and 100) were annealed at 1573 K for 48 h in a vacuum ( $< 2 \times 10^{-3}$  Pa). For neutron irradiation, samples with a 3-mm diameter and 0.25-mm thickness were cut using a wire electric discharge machine. Fe– $x$ Cr ( $x = 30, 45, 50, 70, 85, 91$ , and 100) were annealed at 1273 K for 1 h, and Fe– $x$ Cr ( $x = 0, 9, 15$ ) were annealed at 1073 K for 1 h in a vacuum ( $< 4 \times 10^{-4}$  Pa); both types of samples were water-quenched to suppress phase separation. Neutron irradiation was performed at the Material Controlled Irradiation Facility (SSS) of the Kyoto University Reactor (KUR) [14]. The neutron fluences were  $1.1 \times 10^{22}$ ,  $1.2 \times 10^{22}$ , and  $5.1 \times 10^{22}$  n/m<sup>2</sup> ( $0.44 \times 10^{-3}$ ,  $0.5 \times 10^{-3}$ , and  $2.1 \times 10^{-3}$  dpa) with a displacement threshold energy of 40 eV. The irradiation temperatures were 473 K ( $0.5 \times 10^{-3}$  dpa) and 573 K ( $0.44 \times 10^{-3}$  and  $2.1 \times 10^{-3}$  dpa). All samples were electropolished after neutron irradiation to remove oxidized layers.

Measurements of positron annihilation lifetimes (PAL) and CDB were performed at room temperature. The PAL spectrometer had a time resolution of 190 ps (full width at half maximum) and for each spectrum, a total of  $4 \times 10^6$  counts were accumulated. PAL spectra were analyzed using the PALSfit package [15]. In CDB spectra, low-momentum represents a small Doppler shift resulting from the annihilation of positrons with valence electrons. In this low-momentum region, the counts of the CDB spectra of samples containing vacancy-type defects is higher than those of the defect-free samples. In the high-momentum region, which originates from the annihilation of positrons with core electrons, the counts of CDB spectra in Fe–Cr alloys were heightened in association with the formation of a Fe-rich region [16]. We defined that the S-parameter as the ratio of the low-momentum region ( $|p_L| < 4 \times 10^{-3} m_0c$ ), and the W-parameter as the ratio of the high-momentum region ( $12 \times 10^{-3} m_0c < |p_L| < 28 \times 10^{-3} m_0c$ ) in the Doppler-broadening spectrum to the total region ( $m_0c$ : rest mass of electrons,  $c$ : velocity of light). Vickers hardness tests were conducted using an HMV-T2 (SHIMADZU Corp.) at room temperature with a test load of 0.9807 mN ( $Hv_{0.1}$ ) and a load holding time of 15 s.

## 3. Results and discussion

### 3.1. PAL measurements

Figs. 1–3 show the PAL in Fe–Cr binary alloys irradiated with neutrons at 473 K for 47 h, 573 K for 42 h, and 573 K for 200 h, respectively. The mean positron lifetime ( $\tau_m$ ) denotes the total number of residual defects. The short lifetime component ( $\tau_1$ ) refers to the amount

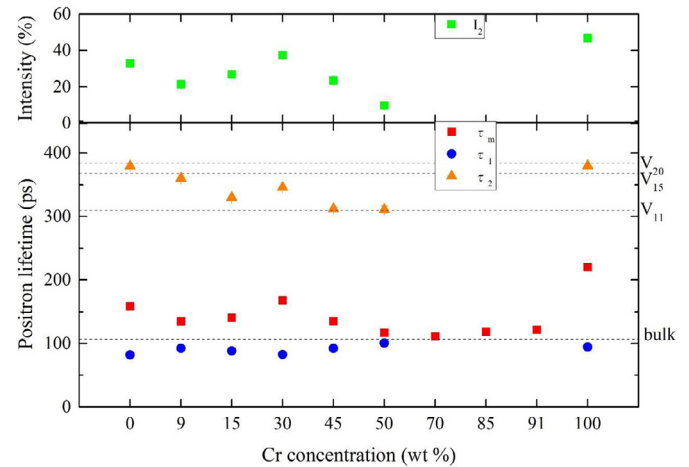


**Fig. 1.** Positron annihilation lifetime in Fe–Cr binary alloys irradiated with neutrons at 473 K for 47 h.

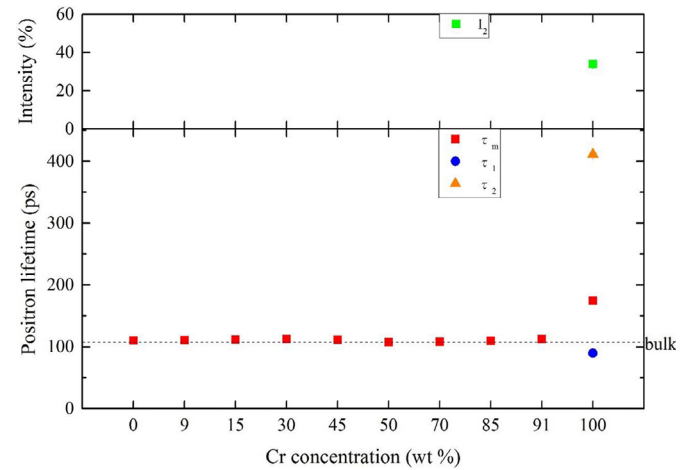


**Fig. 2.** Positron annihilation lifetime in Fe–Cr binary alloys irradiated with neutrons at 573 K for 42 h.

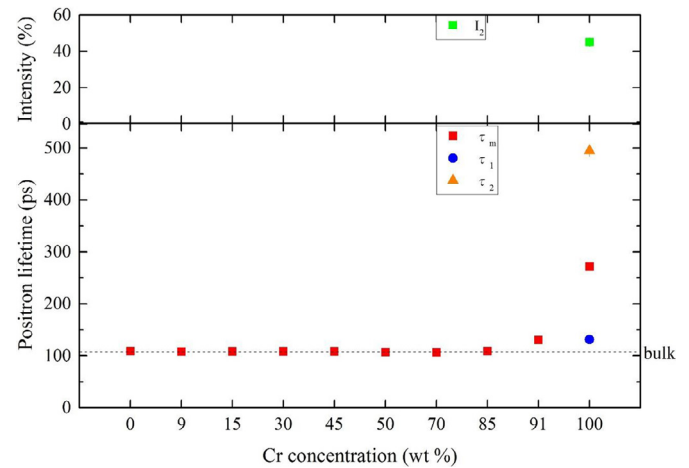


**Fig. 3.** Positron annihilation lifetime in Fe–Cr binary alloys irradiated with neutrons at 573 K for 200 h.

of positron annihilation in the matrix; the long lifetime component ( $\tau_2$ ) denotes the size of vacancy-type defects; the relative intensity of the long lifetime component ( $I_2$ ) corresponds to the density of vacancy-type defects. Vacancy clusters consisting of 8–12 vacancies [17] are formed in the 473 K irradiation except for Fe–70Cr, Fe–85Cr, and Fe–91Cr.

Larger vacancy clusters are detected in pure Fe and Cr. In pure metals, the solute atoms that suppress the migration of vacancies do not exist, resulting in vacancy clusters that are larger than those in alloys. After 573 K irradiation, no vacancy clusters are observed except for pure Cr. Yoshiie et al. reported that the density of vacancy clusters in pure Fe irradiated with neutrons at 473 K was higher than that at 573 K from the results of PAL measurements [18], which correspond to our results. They also indicated that the low density of vacancy clusters was detected after irradiation at 573 K at a dose of  $2.1 \times 10^{-2}$  dpa [18]. In this study, the irradiation doses were lower than in the previous study. Thus, we could not detect vacancy clusters after 573 K irradiation. However, since vacancy clusters were detected in pure Cr, they were more stable in pure Cr than in pure Fe with the high-temperature irradiation. We discuss in Section 3.4 the reason for which we also did not detect vacancy clusters in Fe-70Cr, Fe-85Cr, and Fe-91Cr irradiated at 473 K.

### 3.2. CDB measurements

Kasada et al. detected the progress of phase separation by the CDB measurements in Fe-xCr ( $x = 0, 9, 15, 30, 45, 50, 70, 85, 91$ , and 100) by thermal aging at 748 K [19]. They also investigated the effect of thermal aging on surface hardness [19]. Before thermal aging, when the Fe content was higher, CDB spectra in the high-momentum region heightened (W-parameter increased). In each alloy, the W-parameter and hardness increased after thermal aging at 748 K.

Figs. 4–6 show the CDB ratio curves of neutron-irradiated and unirradiated Fe-9Cr, Fe-50Cr, and Fe-70Cr to unirradiated Cr, respectively. The CDB spectra from the Fe-xCr ( $x = 15, 30, 45$ , and 50) are nearly the same as those of Fe-9Cr; further, those from the Fe-85Cr and Fe-91Cr are similar to those from Fe-70Cr. Therefore, we omitted the curves from Fe-xCr ( $x = 15, 30, 45, 85$ , and 91). The W-parameter is higher after irradiation in Fe-xCr ( $x = 70, 85$ , and 91) irradiated at 473 K and in all Fe-Cr alloys irradiated at 573 K. This indicates that as the Fe-rich phase grew, the number of positrons which were annihilated with the core electrons of the Fe atoms increased.

In Fe-xCr ( $x = 9, 15, 30, 45$ , and 50) irradiated at 473 K, the S-parameter was higher than that of the unirradiated samples because of the formation of vacancy clusters. If the S-parameter increased, the W-parameter relatively decreased because the CDB ratio curves were normalized. In Fe-xCr ( $x = 9, 15, 30, 45$ , and 50) irradiated at 473 K, the decrease in the W-parameter was caused by the increase in the S-

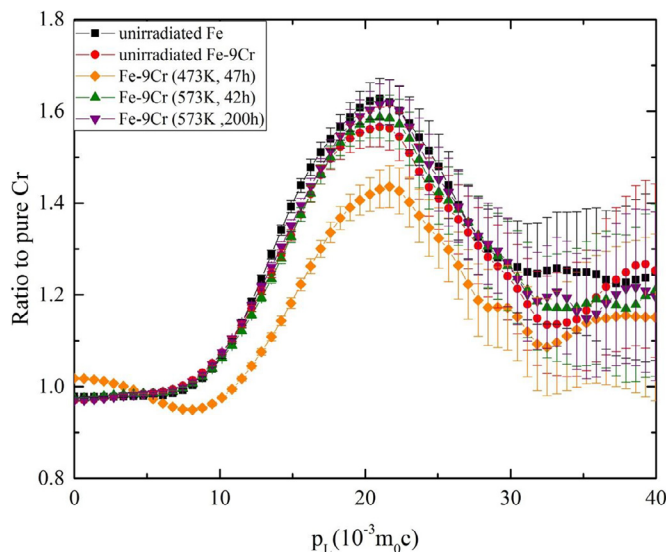


Fig. 4. CDB ratio curves of neutron-irradiated Fe-9Cr alloys to pure Cr. Those of unirradiated pure Fe and Fe-9Cr are also shown.

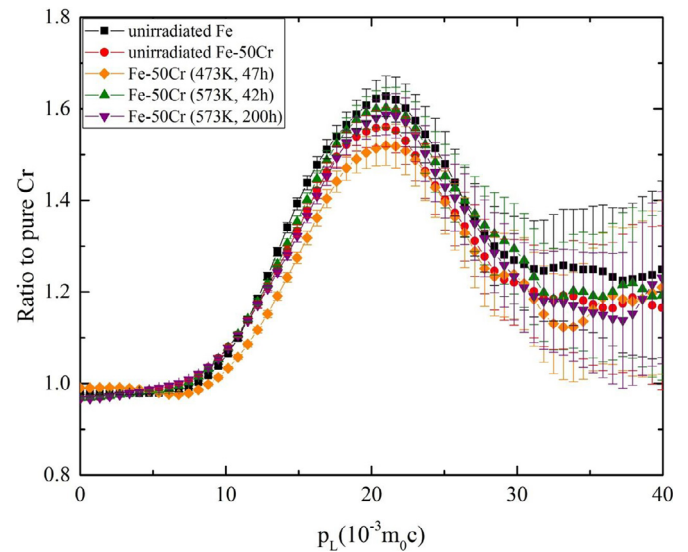


Fig. 5. CDB ratio curves of neutron-irradiated Fe-50Cr alloys to pure Cr. Those of unirradiated pure Fe and Fe-50Cr are also shown.

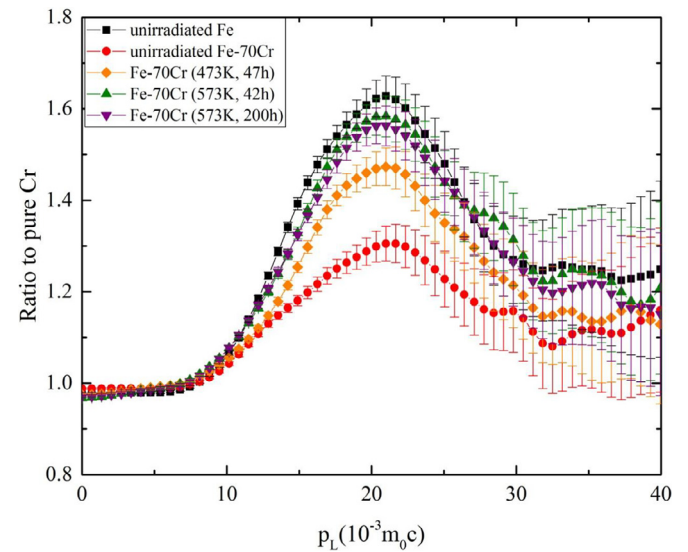


Fig. 6. CDB ratio curves of neutron-irradiated Fe-70Cr alloys to pure Cr. Those of unirradiated pure Fe and Fe-70Cr are also shown.

parameter. Therefore, we cannot be certain that phase separation progresses with only the CDB measurements.

### 3.3. Vickers hardness

Fig. 7 shows the Vickers hardness of Fe-xCr ( $x = 0, 9, 15, 30, 45, 50, 70, 85, 91$ , and 100) irradiated with neutrons at 473 K and 573 K. Data from unirradiated samples are also shown. The hardness increases following neutron irradiation in all samples, due to the progressing phase separation and the formation of irradiation-induced defects. In Fe-xCr ( $x = 0, 9$ , and 15), hardness is highest after 473 K irradiation. Because vacancy clusters are detected in the PAL measurements after 473 K irradiation, the most significant cause of this increase in hardness is the formation of irradiation-induced defects. In Fe-xCr ( $x = 30, 45, 50, 85$ , and 91), the hardness after irradiation at 473 K for 47 h is nearly the same as that of samples irradiated at 573 K for 42 h. The relative contribution of irradiation-induced defects to the increase in the hardness is also different for each sample, as the formation of vacancy clusters is detected by the PAL measurements after irradiation at 473 K.



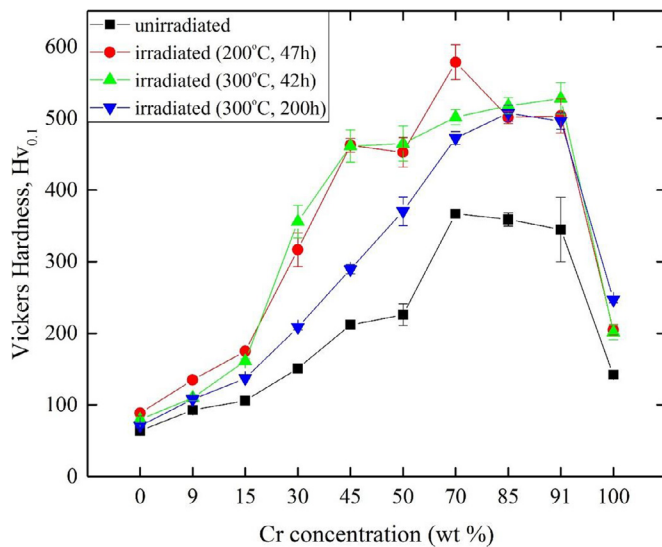


Fig. 7. Vickers hardness of neutron-irradiated Fe–Cr binary alloys. Data from unirradiated samples are also shown.

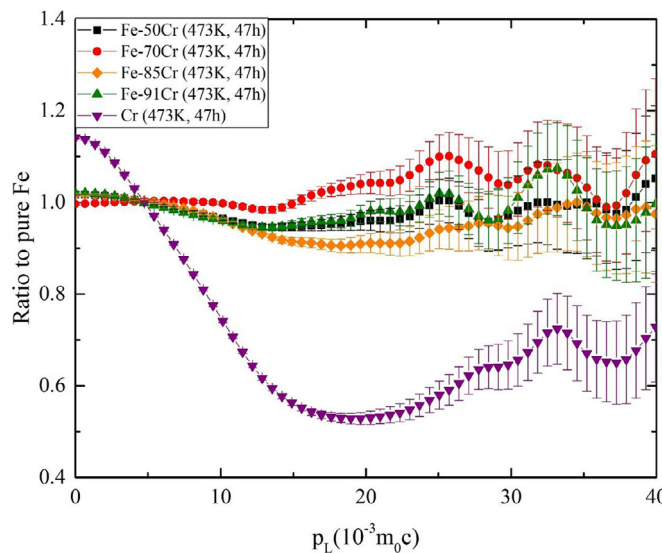


Fig. 8. CDB ratio curves of Fe–xCr ( $x = 50, 70, 85, 91$ , and  $100$ ) irradiated with neutrons at  $473\text{ K}$  for  $47\text{ h}$  to pure Fe.

In Fe–xCr ( $x = 15, 30, 45, 50$ , and  $70$ ) irradiated at  $573\text{ K}$  for  $200\text{ h}$ , the hardness was lower than that at  $573\text{ K}$  for  $42\text{ h}$ . When Fe–Cu alloys were thermally aged, the hardness increased by increasing the density of small Cu precipitates at the first stage; it then decreased with the increase in the size and the decrease in the density at the second stage (aging for an extended time or at high temperature) [20]. Dislocations can migrate easily at the second stage. It is expected that a longer irradiation time leads to considerable progress in phase separation, and the period of Fe/Cr density fluctuation could likewise increase. Consequently, the hardness could decrease. In the future, it is necessary to investigate this possibility using thermal-aged Fe–Cr alloys.

### 3.4. Detection of vacancy clusters and phase separation in Fe–xCr ( $x = 70, 85$ , and $91$ )

Fig. 8 shows the CDB ratio curves from the Fe–50Cr, Fe–70Cr, Fe–85Cr, Fe–91Cr, and Cr irradiated with neutrons at  $473\text{ K}$  to an unirradiated Fe. In the region of the W-parameter, all spectra are nearly flat, which indicates that nearly all positrons are annihilated with the

core electrons of Fe atoms. The identical trends are obtained in Fe–xCr ( $x = 9, 15, 30$ , and  $45$ ). From the PAL measurements, vacancy clusters are not detected in Fe–xCr ( $x = 70, 85$ , and  $91$ ). These results indicate that nearly all positrons are annihilated in the Fe-rich phase, and vacancy clusters do not form in the Fe-rich phase. However, in Fe–xCr ( $x = 0, 9, 15, 30, 45, 50$ , and  $100$ ) irradiated at  $473\text{ K}$ , vacancy clusters are detected in the irradiation at  $473\text{ K}$ . Thus, there remains a possibility that vacancy clusters are formed in Cr-rich phase of Fe–xCr ( $x = 70, 85$ , and  $91$ ), which cannot be detected by the PAS.

Nagai et al. detected the formation of Cu precipitates in rolled Fe–1.0 wt.%Cu alloy by the PAS [21]. When there exist vacancy clusters and Cu precipitates in Fe–Cu alloys, positrons are usually trapped at vacancy clusters with a greater frequency, and then disappear [16]. In Fe–xCr ( $x = 70, 85$ , and  $91$ ) used in this study, the Fe content is far higher than the Cu content in the Fe–Cu alloys used by Nagai et al. Since a high density of Cr-rich phases is formed in neutron-irradiated Fe–16 wt.%Cr [11], Fe-rich phases are also likely to be formed in high concentration in Fe–xCr ( $x = 70, 85$ , and  $91$ ) used in this study. Therefore, if Fe-rich phases are incredibly high, vacancy clusters could not be detected in Fe-rich phases despite the existence of the vacancy clusters in Cr-rich phases. In the future, the size and density of Fe-rich phases should be investigated by atom probe tomography, etc.

The vacancy formation energy in  $\alpha$ -Fe and Cr is  $1.72\text{ eV}$  and  $2.56\text{ eV}$ , respectively [22]. Thus, vacancy clusters are formed more easily in Fe than in Cr under the thermal equilibrium state. However, this contradicts non-formation of vacancy clusters in Fe-rich phases in this study. Meanwhile, vacancy clusters were more stable in pure Cr than in pure Fe with the high-temperature irradiation (see Section 3.1). If vacancy clusters are formed in Cr-rich phase of Fe–xCr ( $x = 70, 85$ , and  $91$ ) because of this high-temperature stability of vacancy clusters in Cr, we should examine it using simulations (molecular dynamics method and so on). In the Fe–70Cr, it is expected that the irradiation-induced defects, which exist in Cr-rich phase, would have a particularly large influence on hardness.

## 4. Summary

PAS and Vickers hardness tests were performed in Fe–Cr binary alloys irradiated with neutrons at  $473\text{ K}$  and  $573\text{ K}$ . The formation of vacancy clusters was detected after  $473\text{ K}$  irradiation with PAL measurements except for the cases of Fe–70Cr, Fe–85Cr, and Fe–91Cr. After  $573\text{ K}$  irradiation, clusters were not detected in any sample except for the pure Cr. The W-parameter increased after irradiation in most samples irradiated at  $573\text{ K}$ , and in Fe–70Cr, Fe–85Cr, and Fe–91Cr alloys irradiated at  $473\text{ K}$ . These results indicate the progress of phase separation by neutron irradiation. Vacancy clusters apparently were not formed in the Fe-rich phase of Fe–xCr ( $x = 70, 85$ , and  $91$ ) irradiated at  $473\text{ K}$ , because most positrons were annihilated with the Fe core electrons based on CDB and vacancy clusters were not detected by PAL. We could not determine whether the vacancy clusters are formed in Cr-rich phase from the results of the PAS. Hardness increased due to the progress of irradiation-enhanced phase separation and irradiation-induced defects. The relative contribution of these to the increase in the hardness was different for each sample.

## References

- [1] R.L. Klueh, K. Ehrlich, F. Abe, J. Nucl. Mater. 191 (1992) 116.
- [2] T. Miyazaki, M. Nakagaki, E.Yajima, J. Japan Inst. Met. 38 (1974) 70.
- [3] M. Akita, Y. Uematsu, K. Tokaji, Y. Fujisawa, J. Soc. Mater. Sci. 58 (2009) 964.
- [4] R.O. Williams, Trans. AIME 212 (1958) 497.
- [5] H. Kuwano, Y. Morooka, J. Japan Inst. Met. 45 (1981) 457.
- [6] H. Kuwano, Trans. Japan Inst. Met. 26 (1985) 721.
- [7] H. Kuwano, Trans. Japan Inst. Met. 26 (1985) 730.
- [8] S.S. Brenner, M.K. Miller, W.A. Soffa, Scripta Metall. 45 (1981) 457.
- [9] M.H. Mathon, Y. de Carlan, G. Geoffroy, X. Averty, A. Alamo, C.H. de Novion, J. Nucl. Mater. 312 (2003) 236.
- [10] M. Hernandez-mayoral, C. Heintze, E. Onorbe, J. Nucl. Mater. 474 (2016) 88.

- [11] W.Y. Chen, Y.B. Miao, Y.Q. Wu, C.A. Tomchik, K. Mo, J. Gan, M.A. Okuniewski, S.A. Maloy, J.F. Stubbins, J. Nucl. Mater. 462 (2015) 242.
- [12] Q. Xu, T. Yoshiie, K. Sato, Philos. Mag. Lett. 88 (2008) 353.
- [13] M.J. Puska, P. Lanki, R.M. Nieminen, J. Phy. Condes. Matter 1 (1989) 6086.
- [14] T. Yoshiie, Y. Hayashi, S. Yanagita, Q. Xu, Y. Satoh, H. Tsujimoto, T. Kozuka, K. Kamae, K. Mishima, S. Shiroya, K. Kobayashi, M. Utsuro, Y. Fujita, Nucl. Instr. Meth. Phys. Res. A 498 (2003) 522.
- [15] J.V. Olsen, P. Kirkegaard, N.J. Pedersen, J. Eldrup, Phys. Stat. Sol. C 4 (2007) 4004.
- [16] Q. Xu, T. Yoshiie, K. Sato, Phys. Rev B 73 (2006) 134115.
- [17] H. Ohkubo, Z. Tang, Y. Nagai, M. Hasegawa, T. Tawara, M. Kiritani, Mater. Sci. Eng. A 350 (2003) 97.
- [18] T. Yoshiie, M. Horiki, Q. Xu, K. Sato, J. Nucl. Mater. 367–370 (2007) 325.
- [19] R. Kasada, K. Sato, to be published.
- [20] T. Yamashita, N. Sano, Z. Chi, M. Enomoto, Y. Shirai, J. Japan Inst. Met. 68 (2004) 1020.
- [21] Y. Nagai, M. Hasegawa, Z. Tang, A. Hempel, K. Yubuta, T. Shimamura, Y. Kawazoe, A. Kawai, F. Kano, Phys. Rev. B 1 (2000) 6574.
- [22] E. de Rio, J.M. Sampedro, H. Dogo, M.J. Caturla, M. Caro, A. Caro, J.M. Perlado, J. Nucl. Mater. 408 (2011) 24.